



ARL-TR-8457 • AUG 2018



A Quasi-Static Indentation Methodology for Screening Ultra-High Molecular Weight Polyethylene Composites for Ballistic Performance

by Jason Cain, Lionel Vargas-Gonzalez, and Mariel Gaviola

Approved for public release; distribution is unlimited.

NOTICES

Disclaimers

The findings in this report are not to be construed as an official Department of the Army position unless so designated by other authorized documents.

Citation of manufacturer's or trade names does not constitute an official endorsement or approval of the use thereof.

Destroy this report when it is no longer needed. Do not return it to the originator.



A Quasi-Static Indentation Methodology for Screening Ultra-High Molecular Weight Polyethylene Composites for Ballistic Performance

by Jason Cain

Survive Engineering, Belcamp, MD

by Lionel Vargas-Gonzalez

Weapons and Materials Research Directorate, ARL

by Mariel Gaviola

Oak Ridge Institute for Science and Education, Oak Ridge, TN

REPORT DOCUMENTATION PAGE

Form Approved
OMB No. 0704-0188

Public reporting burden for this collection of information is estimated to average 1 hour per response, including the time for reviewing instructions, searching existing data sources, gathering and maintaining the data needed, and completing and reviewing the collection information. Send comments regarding this burden estimate or any other aspect of this collection of information, including suggestions for reducing the burden, to Department of Defense, Washington Headquarters Services, Directorate for Information Operations and Reports (0704-0188), 1215 Jefferson Davis Highway, Suite 1204, Arlington, VA 22202-4302. Respondents should be aware that notwithstanding any other provision of law, no person shall be subject to any penalty for failing to comply with a collection of information if it does not display a currently valid OMB control number.

PLEASE DO NOT RETURN YOUR FORM TO THE ABOVE ADDRESS.

1. REPORT DATE (DD-MM-YYYY) August 2018		2. REPORT TYPE Technical Report		3. DATES COVERED (From - To) June 2014–September 2015	
4. TITLE AND SUBTITLE A Quasi-Static Indentation Methodology for Screening Ultra-High Molecular Weight Polyethylene Composites for Ballistic Performance				5a. CONTRACT NUMBER W911QX-16-D-0014	
				5b. GRANT NUMBER	
				5c. PROGRAM ELEMENT NUMBER	
6. AUTHOR(S) Jason Cain, Lionel Vargas-Gonzalez, and Mariel Gaviola				5d. PROJECT NUMBER	
				5e. TASK NUMBER	
				5f. WORK UNIT NUMBER	
7. PERFORMING ORGANIZATION NAME(S) AND ADDRESS(ES) US Army Research Laboratory ATTN: RDRL-WMM-A Aberdeen Proving Ground, MD 21005-5069				8. PERFORMING ORGANIZATION REPORT NUMBER ARL-TR-8457	
9. SPONSORING/MONITORING AGENCY NAME(S) AND ADDRESS(ES)				10. SPONSOR/MONITOR'S ACRONYM(S)	
				11. SPONSOR/MONITOR'S REPORT NUMBER(S)	
12. DISTRIBUTION/AVAILABILITY STATEMENT Approved for public release; distribution is unlimited.					
13. SUPPLEMENTARY NOTES					
14. ABSTRACT Ultra-high molecular weight polyethylene (UHMWPE) composites are an attractive choice for lightweight ballistic resistant materials due to their high mass efficiency, but traditional material characterization test methods are often difficult or unsuitable for this class of materials due to their unique properties. In this effort, a custom test tool has been developed to probe material behavior under quasi-static loading conditions. This tool, which is designed for quasi-static indentation of rigidly backed composite plates, is investigated as an inexpensive and quick ranking tool for evaluating new materials and varying processing conditions. Intriguing insights into the material behavior are gleaned from the correlation of the results with select ballistic results. Results for a number of materials and various processing conditions are presented and are tied to observations of the microstructure obtained from optical microscopy.					
15. SUBJECT TERMS ultra-high molecular weight polyethylene, UHMWPE, quasi-static, indentation, characterization, ballistics					
16. SECURITY CLASSIFICATION OF:			17. LIMITATION OF ABSTRACT UU	18. NUMBER OF PAGES 27	19a. NAME OF RESPONSIBLE PERSON Lionel Vargas-Gonzalez
a. REPORT Unclassified	b. ABSTRACT Unclassified	c. THIS PAGE Unclassified			19b. TELEPHONE NUMBER (Include area code) 410-306-0702

Contents

List of Figures	iv
List of Tables	iv
Acknowledgments	v
1. Introduction	1
2. Experiment	2
2.1 Material Selection	2
2.2 Manufacture and Processing of UHMWPE Composite Plates	3
2.3 Indentation (Quasi-Static and Medium Rate)	4
2.3.1 Quasi-Static Indentation	5
2.3.2 Medium-Rate Indentation Testing	6
2.4 Ballistic Testing	7
2.5 Optical Microscopy	8
3. Results and Discussion	9
3.1 Quasi-Static Indentation and Ballistic Testing	9
3.2 Medium-Rate Indentation Test	14
4. Conclusions	15
5. References	17
List of Symbols, Abbreviations, and Acronyms	19
Distribution List	20

List of Figures

Fig. 1	(Left) Loading nose dimensions in millimeters. (Right) Image of loading nose installed in adapter for connection to loading frame.	5
Fig. 2	Schematic of the quasi-static indentation test procedure	6
Fig. 3	Load–time and displacement–time curves for medium-rate indentation test	7
Fig. 4	Setup for V_{50} test.....	8
Fig. 5	A typical example of load–displacement curve during quasi-static indentation.....	9
Fig. 6	The relationship between the ballistic performance and the peak load from quasi-static indentation tests for SR-3136.....	11
Fig. 7	Correlation between quasi-static and ballistic data.....	11
Fig. 8	Indentation site shown from top, showing portion of top plies (with permanent marker dot) that has been plugged and remains at the bottom of the indentation hole after testing	12
Fig. 9	Cross-section micrograph of a quasi-static indentation site showing plugged top plies remaining at the bottom of the indentation site	13
Fig. 10	Comparison of cross sections from quasi-static indentation (left), and ballistic impact (right).....	14
Fig. 11	Peak load for quasi-static (QS) versus medium-rate (MR) (at 350 mm/s) indentation testing.....	15

List of Tables

Table 1	Material designations, matrix class, and processing conditions considered	3
Table 2	Quasi-static indentation results (peak load), and ballistic results	10

Acknowledgments

The research reported in this document was performed in connection with contract W911QX-16-D-0014 with the US Army Research Laboratory. The views and conclusions contained in this document are those of Service Engineering and the US Army Research Laboratory. Citation of manufacturer's or trade names does not constitute an official endorsement or approval of the use thereof. The US Government is authorized to reproduce and distribute reprints for Government purposes notwithstanding any copyright notation hereon.

1. Introduction

Ultra-high molecular weight polyethylene (UHMWPE) composites are a ballistic material class of interest to the Army due to their low density and high penetration resistance, and therefore, high ballistic efficiency. UHMWPE composites are used in a variety of vehicular and personnel protection applications. The material manufacturers develop new grades every few years, with successive generations of materials attaining higher ballistic efficiencies. In general, the manufacturers achieve much of the performance improvements by increasing the fiber tenacity, which is generally understood to be the primary driver of ballistic efficiency for these materials.¹⁻⁵ Scott⁶ has depicted the chain of events and failure modes associated with small-fragment ballistic impact. In this view, the initial portion of the event is dominated by shear/plugging behavior through a number of initial plies. A transition zone follows as the behavior becomes more strongly affected by membrane-like stretching of the remaining intact plies and leads finally to behavior dominated by membrane stretching. The material is thought to derive its superior ballistic performance primarily from this final phase as this is when the high-tenacity fibers are loaded in tension.

Matrix chemistry, ply thickness, and resin content are among the other manufacturer-driven material parameters that also influence the ballistic performance in significant ways.^{7,8} In addition to material parameters, which are largely out of the hands of end users, researchers or other users can adjust fairly broad ranges of processing parameters to extract the maximum performance from these materials. Processing pressure and temperature are two well-studied examples.⁹⁻¹² Using vacuum or the inclusion of compliant pressure pads during pressing are two other examples of other processing variations that have been investigated by the Army.

However, because of the large number of possible material and processing variables, researchers desire a relatively inexpensive screening test to help guide them in choosing directions for investigation. This report describes a testing methodology that is inspired by ballistic testing, but the use of which under quasi-static conditions is much quicker and less expensive. This method entails the quasi-static penetration of the material with a loading nose modeled on the geometry of a 17-gr (0.22-cal.) fragment-simulating projectile (FSP). The test specimen is a flat, rigidly backed UHMWPE laminate, and the loading nose is driven through most of the specimen's 8-mm thickness. Load-displacement curves are generated and the peak load is used as a discriminating metric.

Despite very different boundary conditions and strain rates between the quasi-static tests and ballistic tests, a significant correlation exists between ballistic resistance to penetration results (V_{50}) and the peak load taken from the quasi-static test output. This report presents the testing methodology and discusses its potential value. Examples of optical micrographs are shown, which provide some insight into failure mechanisms and suggest further information that may be gleaned from this test. Results from the indentation tests at a higher loading rate are also presented to demonstrate rate sensitivity.

2. Experiment

2.1 Material Selection

Many grades of UHMWPE ballistic material are available on the market that are of interest to the US Army. A wide variety of these materials is included in the testing reported here. Several grades with polyurethane-based matrices were tested (hereafter referred to as Group A materials), as were several grades with synthetic rubber-based matrices (Group B materials). Among the latter group were two experimental, noncommercial grades—X131 and X-DARPA—developed as part of the Defense Advanced Research Projects Agency (DARPA) Soldier Protection Systems program in conjunction with an industry partner. Other material grades tested were from 1) DSM (Heerlen, The Netherlands): Dyneema HB25, Dyneema HB26, Dyneema HB80, Dyneema HB50, and Dyneema HB212 and 2) Honeywell Specialty Materials (Morristown, New Jersey): Spectra SR-3124 and Spectra SR-3136. Table 1 lists the shorthand designations of the materials and the processing conditions used. Specimens of materials A4 and B5 (SR-3136 and HB212) were fabricated at five and four different processing pressures, respectively, in order to investigate the effects on ballistic and quasi-static performance of processing pressure changes for materials of the two different matrix types.

Table 1 Material designations, matrix class, and processing conditions considered

Material designation	Matrix type	Manufacturer's designation	Processing temperature (°C)	Processing pressure (MPa)
A1		HB25	125	19.1
A2		HB26	125	19.1
A3		HB80	125	19.1
A4-1	Polyurethane	SR-3136	132	13.8
A4-2		SR-3136	132	20.7
A4-3		SR-3136	132	34.5
A4-4		SR-3136	132	41.4
A4-5		SR-3136	132	69.0
B1		SR-3124	132	19.1
B2		HB50	125	19.1
B3		X131	125	19.1
B4	Synthetic rubber	X-DARPA	125	19.1
B5-1		HB212	125	20.7
B5-2		HB212	125	27.6
B5-3		HB212	125	34.5
B5-4		HB212	125	48.3

2.2 Manufacture and Processing of UHMWPE Composite Plates

All UHMWPE plates were manufactured using a uniaxial hydraulic ram press (model 800H-48-BCLPX, Wabash MPI, Wabash, Indiana) with a maximum load capacity of 7.1 MN. The stack of UHMWPE composite prepreg sheets was pressed in a cross-ply layup between two 6.4-mm-thick aluminum caul plates that were cut to the same lateral dimensions as the laminates. The nominal areal density of all pressed laminates was 7.8 kg/m².

Typical lateral dimensions of the plates used in the testing were 305 × 305 mm, though with some exceptions. Some data came from plates that were made of a material that was no longer available or at pressures no longer attainable using the hydraulic press due to subsequent revised pressure limits. In the former case, clear, nonaffected areas from ballistically tested panels were used for punch testing. In the latter case, the plates were virgin laminates but with lateral dimensions of 150 × 150 mm. In all cases, the punch test locations were chosen such that the damage produced by the tests (including delaminations, fiber pull-in, out-of-plane

deformation) did not overlap with damage from previous tests and did not extend to the edge of the plate, so that each test was assumed to affect only virgin material.

Various temperatures and pressure schedules were used for the materials studied, but all press cycles followed a general pressing schedule as follows. Initially, pressure equal to one quarter of the nominal processing pressure was applied until the measured laminate temperature reached 60 °C. Full pressure was then applied and the plate temperature was ramped up to the nominal processing temperature (as measured with a thermocouple placed at the midplane of the panel, approximately 3 cm in from the center of one edge). Temperature and pressure were held uniform for 1 h, at which point the temperature was ramped down to ambient. To avoid uncontrolled thermomechanical material relaxation, full pressure was held throughout the cooldown process until the plate temperature dropped below 35 °C. All materials from Group B were debulked under vacuum for a short time before pressing, and the vacuum was held throughout the press cycle in order to avoid voids that are otherwise likely to form with these materials in the absence of vacuum.

2.3 Indentation (Quasi-Static and Medium Rate)

The indentation tooling consisted of a loading nose, shaped to mimic the geometry of a 17-gr (0.22-cal.) FSP¹³ used in the ballistic testing, and a holder/adaptor for connection to the loading frame. The loading nose was made from high-speed tool steel, which was through-hardened to HRC 60, and fit in a recess in the adaptor where it was held with a set screw. The length of the loading nose was substantially longer than an FSP to allow for loading into the holder/adaptor, and for penetration into thick composites. The flare at the rear of the standard FSP was not included in the shape of the loading nose. Figure 1 shows overall dimensions for the loading nose and an image of it installed in the holder/adaptor, which screws directly onto the load cell of the load frame. The hardness of the loading nose is higher than the HRC 30 of the FSPs used in the ballistic testing; however, early indentation tests showed that mild steel loading noses at approximately HRC 30 failed in buckling during testing, and the sharp edges of the nose wore excessively even after one test. The hardened loading noses did not exhibit either of these undesirable behaviors. The high hardness of the noses necessitated that they be manufactured using wire electrical discharge machining.

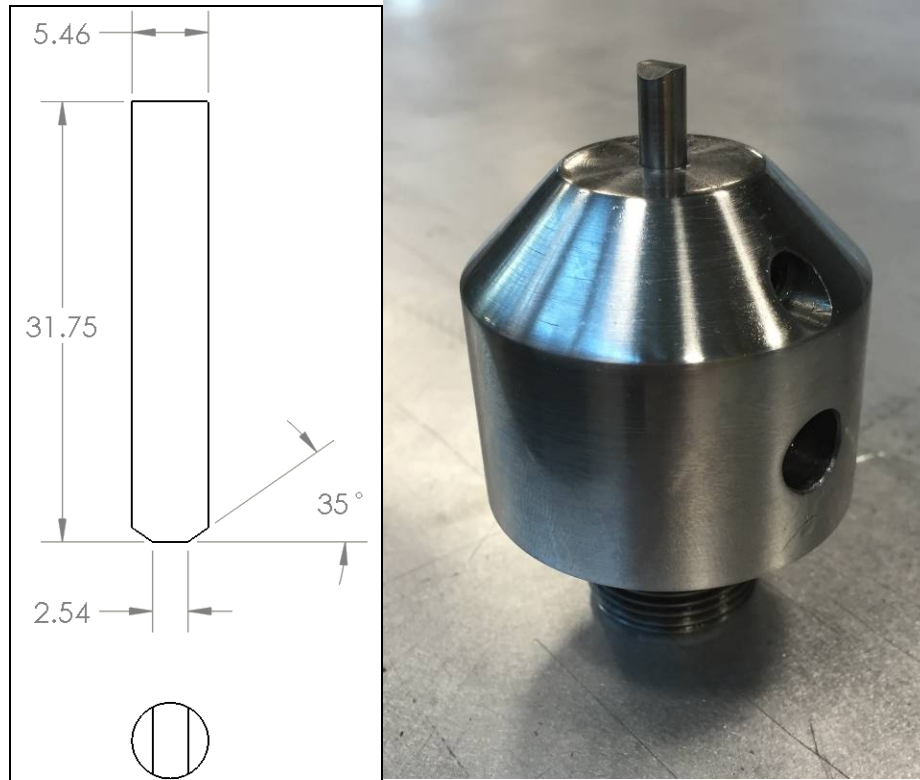


Fig. 1 (Left) Loading nose dimensions in millimeters. (Right) Image of loading nose installed in adapter for connection to loading frame.

2.3.1 Quasi-Static Indentation

For the quasi-static indentation, an Instron 1125 electro-mechanical load frame with a 50-kN load cell (Instron, Norwood, Massachusetts) was used and operated in displacement control mode. The panels were placed flat on a thick, hardened steel platen. Before each test, the loading nose was lowered until it just made contact with the surface of the panel; all subsequent displacements were measured from this datum. The panels were oriented with respect to the loading nose in such a way that the primary fibers of the top layer aligned with the length of the flat tip of the loading nose. Figure 2 is a schematic of the test setup, with the tool shown at the test start position.

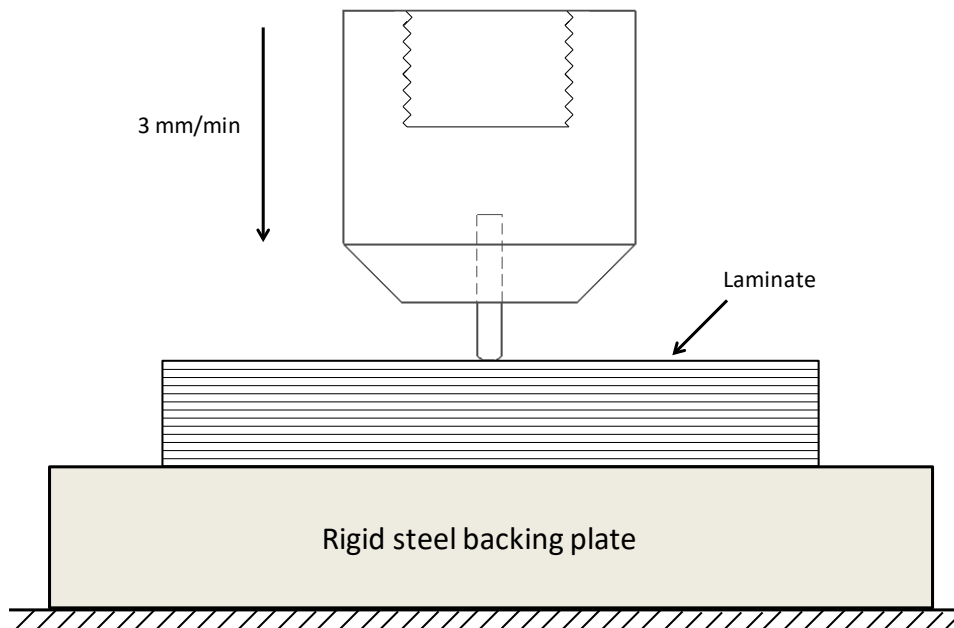


Fig. 2 Schematic of the quasi-static indentation test procedure

The test consisted of driving the loading nose into the composite panel to a depth of 7 mm at a crosshead displacement rate of 3 mm/min. Load and displacement data were collected at 10 Hz. The displacement data were the nominal displacement of the machine crosshead and did not account for machine or tooling compliance, as these were assumed negligible in the context of this test. Ten specimens were tested for each material or processing condition.

From the load–displacement curves that were generated, the largest peak load during the test was used as the metric to assess relative performance.

2.3.2 Medium-Rate Indentation Testing

Medium-rate indentation testing was performed on an MTS 810 servo-hydraulic load frame in displacement-controlled mode and with a 100-kN load cell. Due to the configuration of the load frame, the loading nose/adaptor/load cell portion of the load train was stationary, while the lower platen of the machine, on which rested the hardened steel platen and specimen, was actuated toward the stationary loading nose. A nominal platen speed of 350 mm/s was used. Four materials were chosen for evaluation at medium rate: HB50, HB212, HB80, and SR-3136 (B2, B5-1, A3, and A4-2, respectively.)

In order to ensure a uniform platen speed during the indentation event, the test was initiated with the loading nose approximately 15 mm above the test coupon surface. This arrangement allowed for the lower platen and specimen to accelerate to the

desired test speed before indentation occurred. Subsequent review of the load and displacement curves show that a constant platen speed was achieved before indentation began, and that the platen speed remained near constant during the indentation event (see Fig. 3 for a typical example of a displacement–time curve.) The constant velocity portion of the test lasted through approximately 4.5–5 mm of penetration before the platen began to decelerate to avoid fully penetrating the specimen and crashing the platen into the loading nose.

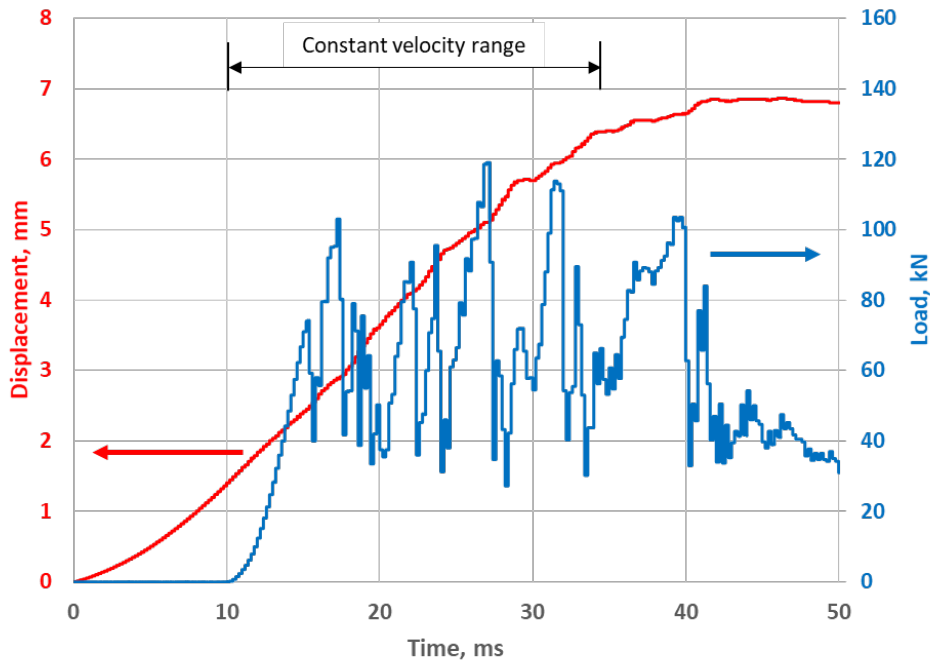


Fig. 3 Load–time and displacement–time curves for medium-rate indentation test

As with the quasi-static indentation case, the largest peak load observed during the test was used as the metric for comparison between materials.

2.4 Ballistic Testing

Ballistic testing was performed using a 17-gr (0.22-cal.) FSP. Target panels were 56 × 56 cm and were lightly clamped to a steel frame with a 25.4- × 25.4-cm square window opening, as shown in Fig. 4. Multiple shots were made into each target; before each shot, the target was positioned such that the desired strike point was positioned at the center of the opening in the frame. Off-axis rotation (yaw) of the FSPs was tracked with high-speed photography, and tests with yaw greater than 5° were disregarded. Shots were not spaced in a prescribed pattern but were spaced sufficiently far from one another to not have overlapping or nearly overlapping damage zones. The extent of damage zones was determined through tap testing and

visual observation in front of a light table. The shots were also spaced sufficiently far from all edges to minimize any edge effects.

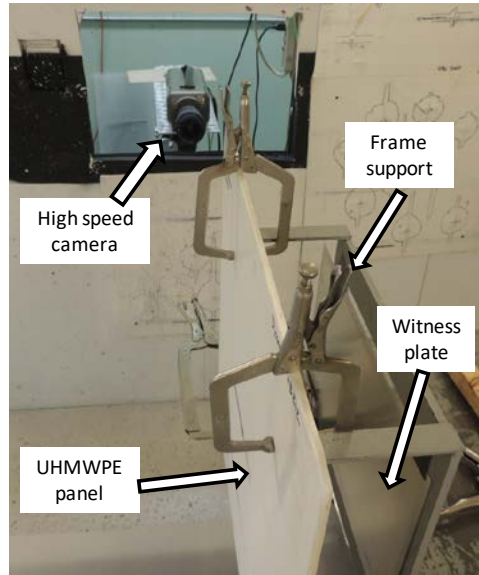


Fig. 4 Setup for V_{50} test

The ballistic limit, V_{50} , for a given set of specimens was determined by taking the arithmetic mean of the striking velocities of an equal number of the highest partial penetrations and lowest complete penetrations.¹⁴ Recorded striking velocities were corrected for drag. Data reported from the testing range included V_{50} numbers and estimates of the sample standard deviation derived from regression analysis.

2.5 Optical Microscopy

For a small number of materials tested quasi-statically, a specimen was sectioned and prepared for optical microscopy to investigate the microstructural evolution during the test. A specimen was also prepared from the impact site of a partial penetration from a ballistic test. Before sectioning, the indentation/impact sites were filled with a Buehler Epo-Color red potting compound (Buehler, Lake Bluff, Wisconsin), which was allowed to cure overnight at room temperature. A waterjet was then used to cut square 19- × 19-mm specimens with one side passing through the center of the indentation site. These specimens were then potted in Struers Epo-Fix potting compound (Struers Inc., Cleveland, Ohio) using potting cups of 31.8-mm diameters.

A Leco Spectrum System 2000 (Leco, St. Joseph, Michigan) autopolisher was used with a nine-specimen, centrally loaded carousel. All polishing was done with all nine specimens loaded, and the lowest possible central load of 22.2 N was selected on the polisher, resulting in a load of approximately 2.5 N per specimen. Various

silicon carbide papers were used, followed by final polishing using alumina slurries down to 0.05 μm . Optical micrographs were prepared using an Olympus MX50 microscope in dark-field mode. Cross-sectional images of the penetration site were composited from a number of smaller images to display the entire area of interest.

3. Results and Discussion

3.1 Quasi-Static Indentation and Ballistic Testing

Figure 5 shows a typical load–displacement curve from the quasi-static indentation testing. The curve clearly shows numerous discrete failure events resulting in a sawtooth pattern. Each failure event corresponded to a loud and sharp acoustic event.

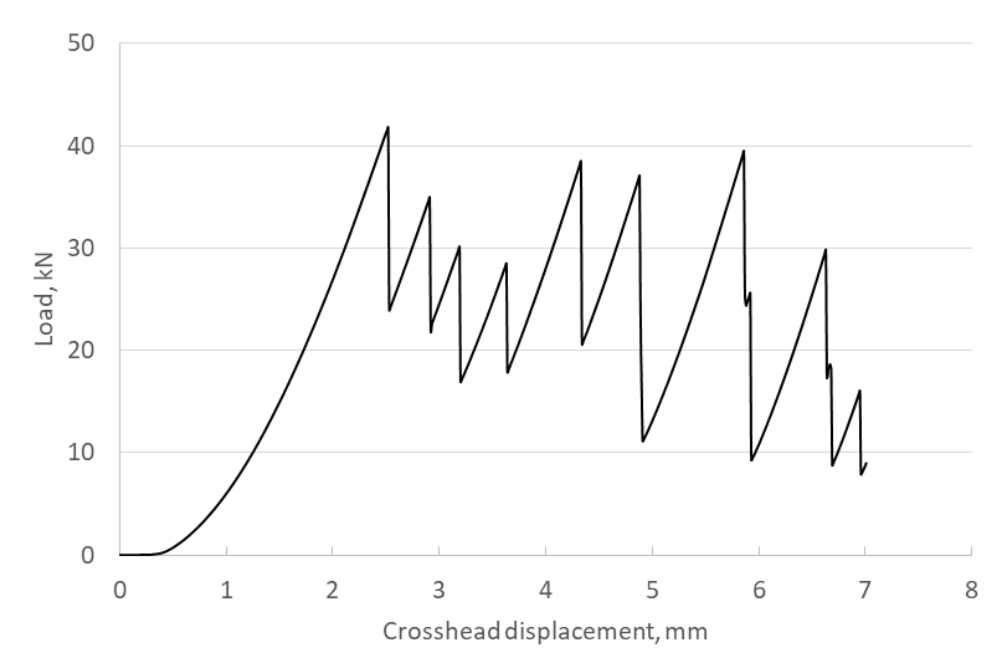


Fig. 5 A typical example of load–displacement curve during quasi-static indentation

Two interesting phenomena were observed in the quasi-static load–displacement curves. First, the initial load peak leading to the first failure of all materials tested exhibited a general tendency to be larger than all subsequent peaks. Second, the number of failure events seen in the load–displacement curve for each specimen was considerably lower than the number of plies of material that were penetrated, suggesting that the plies fail in “packets” of multiple plies.

Table 2 lists the results of both the quasi-static indentation and ballistic tests. (The ballistic results have been normalized with respect to the result for material A4-1.)

The ballistic data for materials A4-1, A4-2, A4-3, A4-4, and A4-5 (Spectra Shield II SR-3136), when processed at escalating pressures, show proportional gains in resistance to both quasi-static and ballistic penetration. Figure 6 shows the quasi-static indentation peak load plotted versus the normalized V_{50} data for this material. Clearly, there is a strong correlation between the mean peak load and V_{50} . For this material, the quasi-static test can be used as a crude ranking indicator of relative performance expected as a function of processing pressure. However, the experimental scatter for the quasi-static indentation peak load is quite large. A similar analysis of materials B5-1, B5-2, B5-3, and B5-4 (Dyneema HB212) indicates that neither that material's quasi-static nor ballistic performance is greatly affected by processing pressure over the range studied.

Table 2 Quasi-static indentation results (peak load), and ballistic results

Material designation	Processing pressure (MPa)	Peak load (kN)		Normalized V_{50}	
		Average	Std dev	Average	Std dev
A1	19.1	31.3	2.8	1.010	0.011
A2	19.1	29.3	2.3	1.010	0.011
A3	19.1	34.2	2.2	1.114	0.015
A4-1	13.8	32.8	2.0	1.000	0.013
A4-2	20.7	33.7	2.0	1.038	0.016
A4-3	34.5	34.9	2.0	1.111	0.010
A4-4	41.4	36.2	1.8	1.167	0.009
A4-5	69.0	37.9	1.9	1.194	0.008
B1	19.1	20.3	1.4	1.063	0.004
B2	19.1	24.1	2.3	1.176	0.020
B3	19.1	39.5	2.1	1.434	0.040
B4	19.1	36.1	1.9	1.482	0.020
B5-1	20.7	40.5	1.2	1.481	0.032
B5-2	27.6	38.8	3.7	1.514	0.021
B5-3	34.5	38.2	1.6	1.508	0.038
B5-4	48.3	40.5	3.5	1.536	0.033

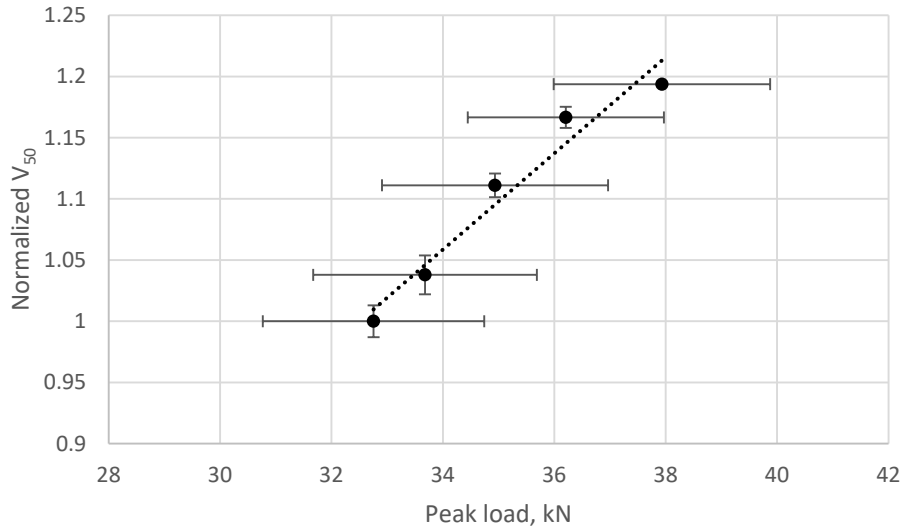


Fig. 6 The relationship between the ballistic performance and the peak load from quasi-static indentation tests for SR-3136

When the quasi-static and ballistic data from Table 2 are plotted in Fig. 7, it becomes apparent that there is a relatively strong correlation seen between the two, and a linear fit can be approximately passed through the data points, provided that Group A and Group B are plotted in separate datasets. This correlation may be a useful tool when investigating the anticipated effects of new materials or changing processing parameters.

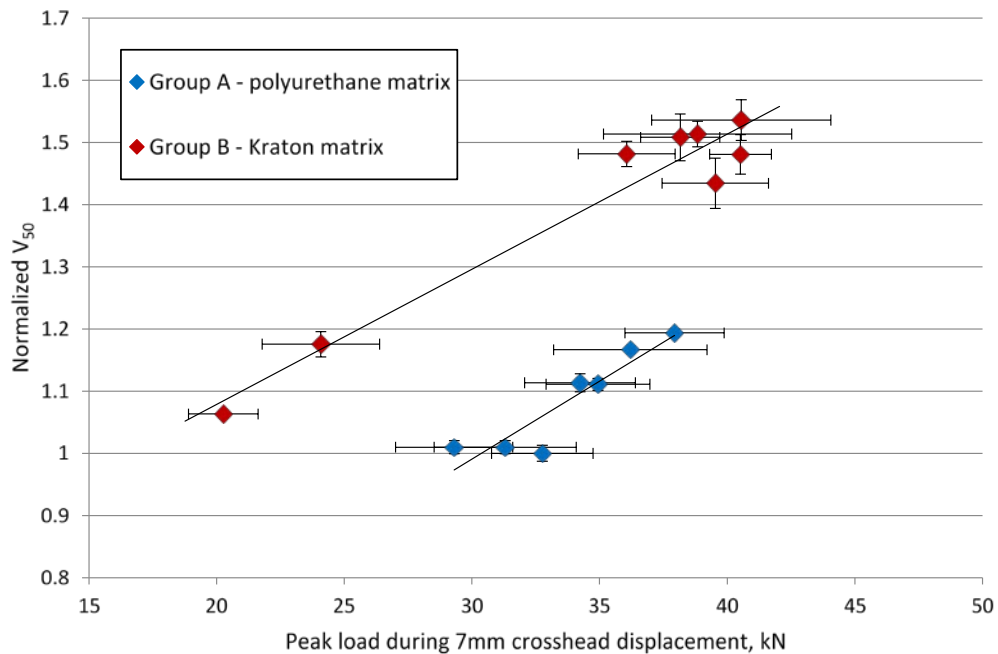


Fig. 7 Correlation between quasi-static and ballistic data

For all materials and for each test, it was observed that a small plug consisting of the top few plies were driven to the bottom of the indentation site (see Fig. 8, in which a permanent marker dot placed on the top surface at the indentation site is seen at the bottom of the indentation hole after the test.) These plugs appeared to be approximately the same diameter as the hole resulting from the indentation, as shown in Fig. 9. This observation suggests that the primary mode of failure for the top few plies is most likely shear plugging. However, there was no indication of any other plugged material or other debris at the bottom of the indent sites, suggesting that a different failure mechanism became predominant for the remaining plies.



Fig. 8 Indentation site shown from top, showing portion of top plies (with permanent marker dot) that has been plugged and remains at the bottom of the indentation hole after testing

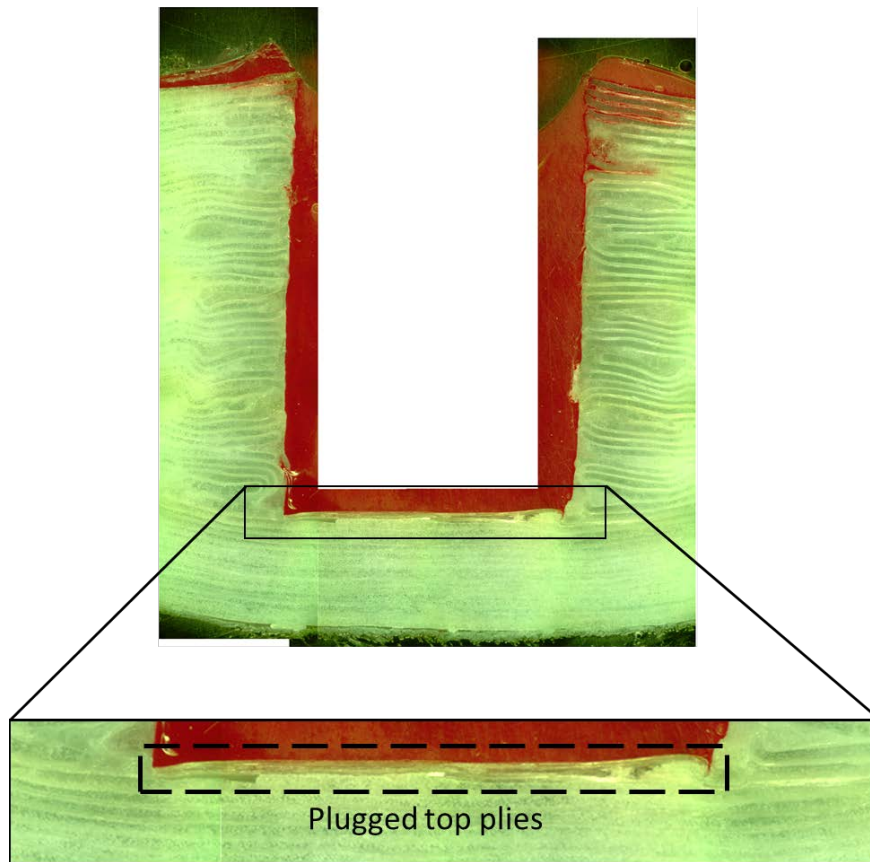


Fig. 9 Cross-sectional micrograph of a quasi-static indentation site showing plugged top plies remaining at the bottom of the indentation site

After the initial shear plugging, it is less clear what failure mechanisms predominate. Attwood et al.¹⁵ have proposed that out-of-plane compressive stress can cause in-plane tension in the material that can build to a sufficient level to cause fiber rupture. Such failure events are quite energy intensive due to the large strength of the UHMWPE fibers. It is possible that such a mechanism is present in the later failure events in the indentation test, as well. This would explain the loud noise and relatively large energies associated with the failures. The stress state in the indentation test, however, is surely more complex than that in Attwood's test and must include some degree of through-thickness shear, as well as other stress components, such as interlaminar shear. Observations from optical microscopy provide some hints as to the behavior during failure. However, a detailed study of the full stress state and failure mechanisms is beyond the scope of this report and will be addressed in a follow-on effort.

Figure 10 shows micrographs from a typical quasi-static test (left) and from a ballistic impact of a 0.22-cal. FSP (right). Both show evidence of shearing of the plies near the top surface, as well as significant delamination, as evidenced by the

penetration of the red potting compound. Below this, the ballistic micrograph shows a transition region (from shear to membrane behavior) in which fibers have buckled, most likely from rebound after fracture and compression from being displaced by the projectile. The quasi-static micrograph shows evidence of buckling as well over the rest of the length of penetration. The regular appearance of these buckled plies are further evidence of the failure of plies in discrete packets, rather than individually.

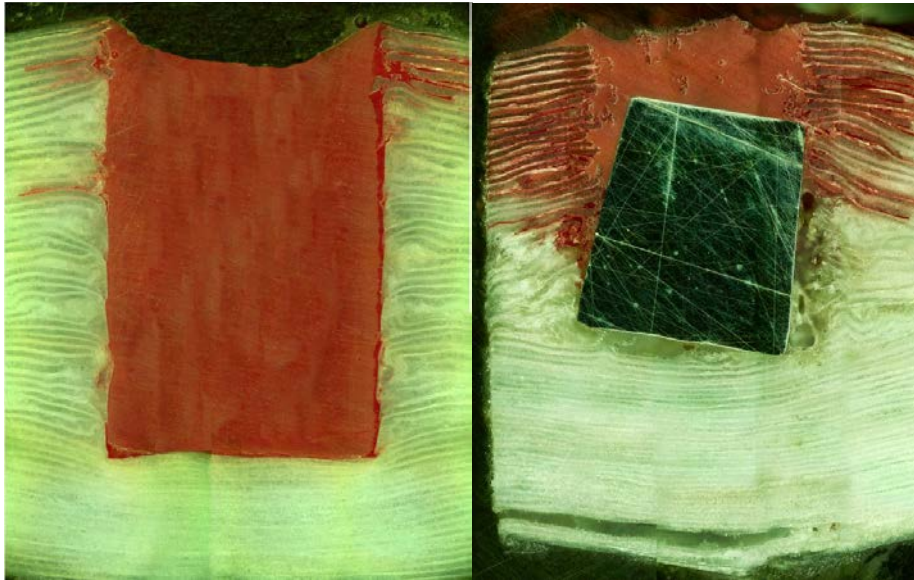


Fig. 10 Comparison of cross sections from quasi-static indentation (left), and ballistic impact (right)

3.2 Medium-Rate Indentation Test

Figure 11 shows a comparison of the average peak load seen during quasi-static and medium-rate dynamic indentation tests for the four materials evaluated at medium rate. All four materials experienced a decrease in peak load when tested at medium rate compared to quasi-static testing, though the two materials with Kraton matrices (HB50/B2 and HB212/B5-1) experienced only small apparent decreases of 5.3% and 5.7%, respectively, that fall well within the experimental scatter. The two materials with the polyurethane matrices (HB80/A3 and SR-3136/A4-3), however, experienced significantly larger decreases in peak load of 17.7% and 30.1%, respectively. This rate sensitivity is most likely driven by matrix effects. Russell et al.¹⁷ have shown the rate sensitivity of UHMWPE fibers and yarns is very low for strain rates up to 10^3 s^{-1} , which is well above the strain rate seen during the medium-rate indentation.

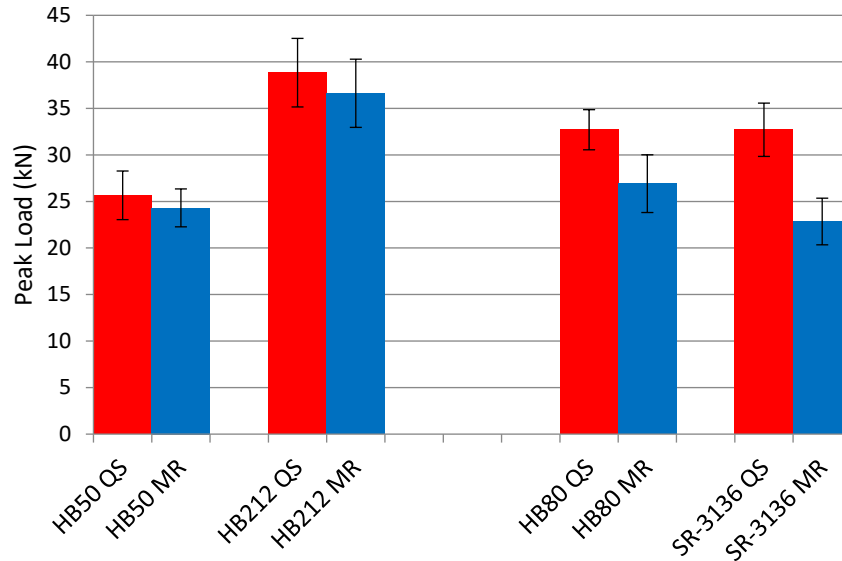


Fig. 11 Peak load for quasi-static (QS) versus medium-rate (MR) (at 350 mm/s) indentation testing

4. Conclusions

A quasi-static indentation methodology has been developed for use in screening new UHMWPE materials and processing methods in an efficient and inexpensive way. The indentation test uses a loading nose with the same geometry as a 17-gr FSP commonly used in ballistic tests, but the test coupon is rigidly backed unlike typical ballistic tests. Nevertheless, despite these boundary condition differences, a good correlation between the maximum load seen during the indentation test and the V_{50} from the ballistic tests is observed when the materials are separated into two groups based on the type of matrix (i.e., Kraton or polyurethane.)

Load–displacement curves from the tests show that the material fails in numerous, discrete failure events. Micrographs of sectioned penetration sites demonstrated some qualitative similarities, as well as significant differences, between the resulting microstructure in the quasi-static and ballistic rate cases. These micrographs coupled with the load-displacement data from the quasi-static case provide some clues to the failure mechanisms in that low-rate case, suggesting that after the initial shear plugging, subsequent plies of material fail in “packets” rather than individually.

Medium-rate tests showed that the indentation test is significantly rate sensitive. An increase in the test speed from 3 mm/min to 350 mm/s resulted in reductions in peak load of approximately 5% for Kraton-matrix materials and between 18% and 30% for two polyurethane-matrix materials. This result suggests that care must be

taken to use a consistent test speed when comparing results from different materials or processing conditions.

The quasi-static indentation methodology appears to provide a simple, inexpensive screening tool for researchers investigating new materials and process strategies.

5. References

1. Cunniff PM. Dimensional parameters for optimization of textile-based body armor systems. Proceedings of the 18th International Symposium of Ballistics; 1999; San Antonio, TX.
2. Phoenix SL, Porwal PK. A new membrane model for the ballistic impact response and V50 performance of multi-ply fibrous systems. *International Journal of Solids and Structures*. 2003;40:6723–6765.
3. Woodward RL, Egglestone GT, Baxter BJ, Challis K. Resistance to penetration and compression of fibre-reinforced composite materials. *Composites Engineering*. 1994;4(3):329–335,337–341.
4. Scott B, Cheeseman BA. The mechanics of projectile arrest for compliant cross plied unidirectional laminates. *International Symposium of Ballistics*; 2008 Sep 22–26; New Orleans, LA.
5. Heisserer U, Van der Werff H. The relation between Dyneema fiber properties and ballistic protection performance of its fiber composites. In: Govaert L, editor. *15th International Conference on Deformation, Yield and Fracture of Polymers*. Kerkrade (Netherlands): Technical University Eindhoven; 2012.
6. Scott B. Unusual transverse compression response of non-woven ballistic laminates. *Proceedings of the 26th International Symposium on Ballistics*; 2011 Sep 12; Miami, FL.
7. Lee BL, Walsh TF, Won ST, Patts HM, Song JW, Mayer AH. Penetration failure mechanisms of armor-grade fiber composites under impact. *Journal of Composite Materials*. 2001;35(18):1605–1633.
8. Karthikeyan K, Russell BP, Fleck NA, O'Masta MR, Wadley HNG, Deshpande VS. The soft impact response of composite laminate beams. *International Journal of Impact Engineering*. 2013;60:24–36.
9. Lassig TR, May M, Heisserer U, Riedel W, Bagusat F, van der Werff H, Hiermaier SJ. Effect of consolidation pressure on the impact behavior of UHMWPE composites. *Composites Part B*. 2018;147:47–55.
10. Freitas CJ, Bigger RP, Scott N, LaSala V, MacKiewicz J. Composite materials dynamic back face deflection characteristics during ballistic impact. *Journal of Composite Materials*. 2014;48:1475–1486.

11. Greenhalgh ES, Bloodworth VM, Iannuci L, Pope D. Fractographic observations on Dyneema composites under ballistic impact. *Composites Part A*. 2013;44:51–62.
12. Vargas-Gonzalez LR. Ballistic modification of ultra-high molecular weight polyethylene composites through processing. *Proceedings of the SAMPE 2015 Conference of the Society for the Advancement of Materials and Process Engineering*; 2015 May 18–21; Baltimore, MD.
13. MIL-DTL-46593B. (MR) w/ Amendment 1. Detail specification: projectile, calibers .22, .30, .50, and 20 mm fragment-simulating. Aberdeen Proving Ground (MD): Army Research Laboratory (US), Weapons and Materials Research Directorate; 2008 Aug 11.
14. MIL-STD-662F. Military standard: V50 ballistic test for armor. Aberdeen Proving Ground (MD): Army Research Laboratory (US), Weapons and Materials Research Directorate; 1997 Dec 18.
15. Attwood JP, Khaderi SN, Karthikeyan K, Fleck NA, O’Masta MR, Wadley HNG, Deshpande VS. The out-of-plane compressive response of Dyneema composites. *Journal of Mechanics and Physics of Solids*. 2014;70:200–226.
16. Russell BP, Karthikeyan K, Deshpande VS, Fleck NA. The high strain rate response of ultra-high molecular weight polyethylene: from fibre to laminate. *International Journal of Impact Engineering*. 2013;60:1–9.

List of Symbols, Abbreviations, and Acronyms

DARPA	Defense Advanced Research Projects Agency
FSP	fragment-simulating projectile
MR	medium-rate
QS	quasi-static
UHMWPE	ultra-high molecular weight polyethylene

1 DEFENSE TECHNICAL
(PDF) INFORMATION CTR
DTIC OCA

2 DIR ARL
(PDF) IMAL HRA
RECORDS MGMT
RDRL DCL
TECH LIB

1 GOVT PRINTG OFC
(PDF) A MALHOTRA

3 NSRDEC
(PDF) D COLANTO
R DILALLA
T KAYHART

1 PEO SOLDIER
(PDF) A FOURNIER

13 ARL
(PDF) RDRL WMM A
J CAIN
J SANDS
J TZENG
D O'BRIEN
T BOGETTI
C YEN
A QUABILI
E WETZEL
M GAVIOLA
RDRL WMM E
L VARGAS-GONZALEZ
S SILTON
RDRL WMP B
C HOPPEL
RDRL WMP D
B SCOTT